

# DISCOVERY OF A 66 mas ULTRACOOL BINARY WITH LASER GUIDE STAR ADAPTIVE OPTICS<sup>1</sup>

NICK SIEGLER,<sup>2</sup> LAIRD M. CLOSE,<sup>2</sup> ADAM J. BURGASSER,<sup>3</sup> KELLE L. CRUZ,<sup>4,5</sup> CHRISTIAN MAROIS,<sup>6</sup>  
BRUCE MACINTOSH,<sup>6</sup> AND TRAVIS BARMAN<sup>7</sup>

Received 2006 December 28; accepted 2007 January 26

## ABSTRACT

We present the discovery of 2MASS J21321145+1341584AB as a closely separated (0.066"), very low mass field dwarf binary, resolved in the near-infrared by the Keck II telescope using laser guide star adaptive optics. Physical association is deduced from the angular proximity of the components and constraints on their common proper motion. We have obtained a near-infrared spectrum of the binary and find that it is best described by an  $L5 \pm 0.5$  primary and an  $L7.5 \pm 0.5$  secondary. Model-dependent masses predict that the two components straddle the hydrogen-burning limit threshold, with the primary likely stellar and the secondary likely substellar. The properties of this system—close projected separation ( $1.8 \pm 0.3$  AU) and near-unity mass ratio—are consistent with previous results for very low mass field binaries. The relatively short estimated orbital period of this system ( $\sim 7$ – $12$  yr) makes it a good target for dynamical mass measurements. It is interesting to note that the system's angular separation is the tightest yet for any very low mass binary published from a ground-based telescope and that it is the tightest binary discovered with laser guide star adaptive optics to date.

*Key words:* binaries: visual — stars: individual (2MASS J21321145+1341584) — stars: low-mass, brown dwarfs

*Online material:* color figure

## 1. INTRODUCTION

The coolest and lowest mass objects have historically been discovered as companions to low-luminosity stars. These objects include the two lowest luminosity spectral classes of low-mass stars and brown dwarfs: the L and T dwarfs (Kirkpatrick 2005 and references within). The first L dwarf, GD 165B, was discovered as the companion to a white dwarf (Becklin & Zuckerman 1988), while the first widely accepted brown dwarf, Gliese 229B, was the companion to an M dwarf (Nakajima et al. 1995; Oppenheimer et al. 1995). Hence, it is quite possible that the first of the ultracool brown dwarfs with effective temperatures less than  $\sim 700$  K will also be discovered as a companion. These objects would likely populate a new spectral type beyond T, with masses overlapping the planetary regime.

The hunt today for even cooler objects benefits from advances in high-resolution imaging with the *Hubble Space Telescope* (*HST*) and large ground-based telescopes fitted with adaptive optics (AO). With the spectral energy distributions of these cool objects peaking in the near-infrared ( $1$ – $6$   $\mu\text{m}$ ), observing at these wavelengths is advantageous for their detection and characterization. Thus, observational strategies have relied on targeting continuously lower luminosity objects to further improve the contrast differential obtained in the near-infrared.

An advantage in using AO over the *HST* is that AO can be attached to larger ground-based telescopes attaining higher angular resolution and increased sensitivity to fainter sources. The challenge, however, exists in locating natural guide stars suffi-

ciently bright ( $R \lesssim 13.5$  mag,  $K_s \lesssim 12$  mag) and near one's science target (isoplanatic angular distance  $\lesssim 30''$ ) to provide sufficient wave-front correction. There is less than a 10% chance of finding a natural guide star (NGS) meeting these requirements at  $30^\circ$  Galactic latitude (Roddier 2004). The probability improves little, even with the use of infrared wave-front sensors when targeting ultracool objects such as mid-L dwarfs (limiting magnitude of the NGS infrared wave-front sensor on the Nasmyth Adaptive Optics System<sup>8</sup> at the Very Large Telescope is  $K_s \sim 12$  mag). Slightly better NGS sensitivity performance has been achieved using curvature wave-front sensors with avalanche photodiodes where  $K_s \lesssim 12.3$  mag (Siegler et al. 2003).

The search for substellar and planetary-mass objects through direct detection from ground-based telescopes now has a new technique: laser guide stars (LGSs). LGSs serve as artificial beacons for AO systems by exciting sodium atoms in the Earth's mesosphere at their resonant D-line frequency. These beacons serve as artificial (and steerable) guide stars that provide sufficient flux density for wave-front sensing and correcting. While LGS AO still requires a NGS to help correct both the lowest wave-front orders ("tip-tilt,"  $\sim 2$  kHz) and the higher orders ("low-band wave-front sensor,"  $\sim 0.01$  Hz), its flux density requirement is comparatively small ( $R \lesssim 18$  mag). This results in  $\sim \frac{2}{3}$  of the night sky accessible to high spatial resolution imaging (Liu 2006) and opens the door to probing the regions around ultracool L and T dwarfs never previously observed by ground-based telescopes.

While the Keck II is the first of the 8–10 m class telescopes to have an operational LGS AO system (Wizinowich et al. 2006), several more are expected to be commissioned within just the next 2 years (see Liu 2006). Several recent investigations using Keck II LGS AO have discovered companions to previously unresolved faint sources, ushering in this new era of high-resolution imaging (e.g., Liu & Leggett 2005; Gelino et al. 2006; Liu et al. 2006; Close et al. 2007).

<sup>1</sup> Based on observations made with the Keck II telescope.

<sup>2</sup> Steward Observatory, University of Arizona, Tucson, AZ 85721, USA.

<sup>3</sup> Massachusetts Institute of Technology, Kavli Institute for Astrophysics and Space Research, Cambridge, MA 02139, USA.

<sup>4</sup> Department of Astrophysics, American Museum of Natural History, New York, NY 10024, USA.

<sup>5</sup> NSF Astronomy and Astrophysics Postdoctoral Fellow.

<sup>6</sup> Institute of Geophysics and Planetary Physics L-413, Lawrence Livermore National Laboratory, Livermore, CA 94550, USA.

<sup>7</sup> Lowell Observatory, Flagstaff, AZ 86001, USA.

<sup>8</sup> See <http://www.eso.org/instruments/naco/inst/naos.html>.

TABLE 1  
ULTRACOOL FIELD DWARFS OBSERVED WITH NO PHYSICAL  
COMPANION DETECTIONS

Name	$K_s$	Spectral Type	References
LSR J1610–0040 .....	12.02	sdM:sdL:	1, 2
2MASS J17210390+3344160.....	12.47	L3	3
SDSS J202820.32+005226.5.....	12.79	L3	4
2MASS J20343769+0827009 <sup>a</sup> .....	13.08	M:L	5
2MASS J22490917+3205489 <sup>b</sup> .....	13.59	L5	6

NOTES.—For near-equal-mass binaries (mass ratio  $\geq 0.7$ ), the angular separation sensitivity is  $\sim 50$  mas. For less massive companions ( $q \lesssim 0.7$ ), sensitivity improves with increasing angular separation up to our observation’s  $10''$  radial field of view. Each target has at least one bright NGS  $\lesssim 30''$  serving as the tip-tilt and low-band source.

<sup>a</sup> Object was originally classified as a mid-L dwarf, but due to insufficient S/N is now only roughly estimated as a late-M/early-L dwarf.

<sup>b</sup> A faint point source at P.A. =  $194^\circ$  with separation  $\sim 90$  mas was observed in  $J$ ,  $H$ , and  $K_s$ , but it was determined to be a “superspeckle” due to its wavelength-dependent angular separation.

REFERENCES.—(1) Lépine et al. 2003; (2) Cushing & Vacca 2006; (3) Cruz et al. 2003; (4) Hawley et al. 2002; (5) K. Cruz 2006, private communication; (6) Cruz et al. 2007.

In this investigation we observe six nearby ultracool<sup>9</sup> field dwarfs, which we target for very faint companions. The objects were selected from the literature, satisfying the following criteria: spectral type later than M6, never observed at high spatial resolution, too faint for current ground-based NGS AO systems, and spectrophotometric distances less than 30 pc. We present here the discovery of one of the targets, 2MASS J21321145+1341584 (Cruz et al. 2007), as a closely separated ( $0.066''$ ) L dwarf binary resolved by the Keck II telescope NIRC2 infrared camera in combination with LGS AO. The binary is hereafter referred to as 2M 2132+1341AB. The five other targets not found with near-equal-mass companions are listed in Table 1. This discovery demonstrates the power of LGS AO: the ability to resolve a faint ( $R \gtrsim 20$  mag,  $J \sim 16$  mag) binary very near the diffraction limit (50 mas) of a 10 m telescope using an artificial beacon for wavefront correction.

## 2. OBSERVATIONS AND DATA REDUCTION

### 2.1. Imaging

The discovered binary system 2M 2132+1341AB was observed on UT 2006 June 17 with the 10 m Keck II telescope on Mauna Kea, Hawaii. It was the lone binary discovered from our sample of six ultracool dwarf targets. To optimize the resolution capabilities of our observations, we used the facility IR camera NIRC2 in the narrow ( $0.01'' \text{ pixel}^{-1}$ ) camera mode with a  $10'' \times 10''$  field of view, in combination with the sodium LGS AO system (Bouchez et al. 2004; Wizinowich et al. 2004). All targets were observed through the broadband  $K_s$  filter ( $2.15 \mu\text{m}$ ), where Strehl ratios are improved over  $J$  ( $1.25 \mu\text{m}$ ) and  $H$  ( $1.63 \mu\text{m}$ ). In the case of 2M 2132+1341AB, observations were also made in both  $J$  and  $H$ . All filters are from the Mauna Kea Observatories (MKO) filter consortium (Simons & Tokunaga 2002; Tokunaga et al. 2002). Conditions were photometric for the majority of the night, with better than  $0.6''$  seeing in the optical but with occasional windy periods.

Higher order AO corrections were produced using the laser’s on-axis light in the direction of the science target. This produced an emission similar to a  $V \approx 10$  point source. Lower order tip-tilt corrections were obtained using NGSs within  $60''$  of the targets.

In the case of 2M 2132+1341AB, the NGS used was 1036–0598908 ( $R = 14.2$  mag) from the USNO-B1.0 catalog (Monet et al. 2003), located  $13.6''$  away.

Table 1 lists the five ultracool dwarf targets observed with no near-unity mass ratio companions detected at separations  $\gtrsim 0.05''$ . Figure 1 shows the resolved discovered binary 2M 2132+1341AB. Both components are elongated along the telescope elevation axis projected to  $\approx 45^\circ$ , attributed to wind shake during the observations (a common problem with LGS AO on windy nights; see also Liu et al. 2006). The LGS AO-corrected images have full width at half-maxima of  $0.06''$ ,  $0.07''$ , and  $0.07''$  at  $J$ ,  $H$ , and  $K_s$ , respectively.

Each of the images shown in Figure 1 was made by dithering a few arcseconds over three different quadrant positions on the NIRC2 narrow camera detector. Three images were taken per filter per dither position, resulting in 2.5 minutes of total on-source integration time per filter. The object was easily resolved into two components in all our data.

The images were reduced in a consistent manner using an AO data reduction pipeline written in the IRAF language, as first described in Close et al. (2002). Modified for the NIRC2 narrow camera, the pipeline produces final unsaturated  $15'' \times 15''$  exposures in  $J$ ,  $H$ , and  $K_s$  with the highest signal-to-noise ratio (S/N) in the inner  $5'' \times 5''$  region. The photometric reduction pipeline uses the IRAF task ALLSTAR in the DAOPHOT point-spread function (PSF) fitting photometry package.<sup>10</sup> The central regions of the pipeline’s output are shown in Figure 1.

Two different, unsaturated, single objects observed during the same night, but from a different program, were selected as PSF stars. These objects were observed with the same instrumental setup and showed similar Strehl ratios, FWHM, elongation due to wind shake, and air mass. Both PSF sources, incidentally, are resolved primary objects of newly discovered wide ( $1.7''$ – $1.9''$ ) binaries. In both cases, the A and B components are sufficiently separated such that there is no flux contamination between them. The two PSFs used are 2MASS J16233609–2402209A, also shown in Figure 1, and 2MASS J16223020–2322240A (Close et al. 2007). 2M 2132+1341AB was fit independently with both PSF objects, leaving behind clean residuals. The differential photometry in magnitudes is reported in Table 2, and the photometric uncertainties are produced from the differences in the photometry between the two PSFs. These dominate the overall uncertainty.

### 2.2. Spectroscopy

Unresolved, low-resolution, near-infrared spectroscopy of 2M 2132+1341AB was obtained on 2005 October 17 (UT) using the SpeX spectrograph mounted on the 3 m NASA Infrared Telescope facility (Rayner et al. 2003). Conditions during the night were clear, with moderate seeing ( $0.7''$ – $1.0''$  at the  $J$  band). Data were obtained using the SpeX prism mode, providing a single-order spectrum spanning  $0.8$ – $2.5 \mu\text{m}$ , with a dispersion of  $20$ – $30 \text{ \AA pixel}^{-1}$ . Use of the  $0.5''$  slit, aligned with the parallactic angle, provided resolution  $\lambda/\Delta\lambda \approx 120$  across the near-infrared band. Six exposures of 2M 2132+1341AB were obtained in an ABBA dither pattern along the slit, with individual exposure times of 150 s. The system was observed at an air mass of 1.02. The AO star HD 210501 was observed immediately after the target exposures at a similar air mass, followed by internal flat-field and Ar arc lamps for pixel response and wavelength calibration.

Data were reduced using the SPEXTOOL package, version 3.2 (Cushing et al. 2004). The raw science data were processed by performing linearity corrections, pairwise subtraction, and division by

<sup>9</sup> Generally defined as objects with spectral types later than M6 ( $T_{\text{eff}} \lesssim 2700$  K; Kirkpatrick et al. 1995; Dahn et al. 2002).

<sup>10</sup> IRAF is distributed by the NOAO, which is operated by the AURA, Inc., under cooperative agreement with the NSF.

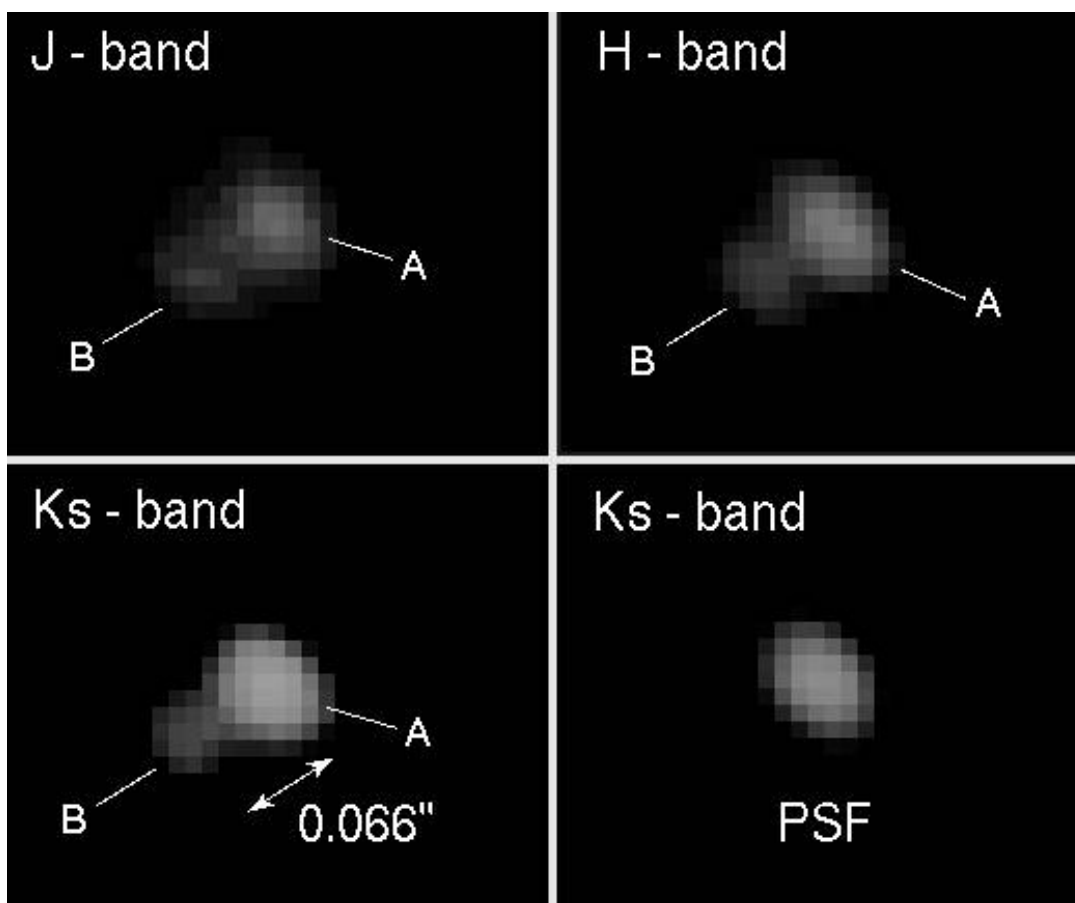


FIG. 1.— $JHK_s$ -band images of 2M 2132+1341AB observed with Keck LGS AO; north is up, and east to the left. We refer to the brighter component as the primary, and we designate it 2M 2132+1341A; the fainter component is referred to as the secondary or the companion, and we designate it 2M 2132+1341B. The angular separation is only  $66 \pm 4$  mas, among the tightest ultracool binaries ever resolved and the tightest yet resolved using a ground-based telescope. The LGS AO-corrected images have full width at half-maxima of  $0.06''$ ,  $0.07''$ , and  $0.07''$  at  $J$ ,  $H$ , and  $K_s$ , respectively. Each image is  $0.3''$  on a side. The binary components are all slightly elongated along the telescope elevation axis (P.A.  $\sim 45^\circ$ ), believed to be due to telescope wind shake. Also shown is one of the two PSFs used in the data reduction, 2MASS J16233609–2402209A (Close et al. 2007), a young, stellar mass M5 observed with similar elongation and air mass. [See the electronic edition of the *Journal* for a color version of this figure.]

a normalized flat field. The spectra were then extracted using the SPEXTOOL default settings for point sources, and wavelength solutions were calculated using the Ar arc calibration frames. Extracted spectra from the same source were scaled to match the highest S/N spectrum of the set, and the scaled spectra were median-combined. Telluric and instrumental response features were removed following the procedure of Vacca et al. (2003).

The reduced spectrum of 2M 2132+1341AB is shown in Figure 2 (*black line*). Strong absorption features of  $H_2O$  are present at 1.4 and  $1.9 \mu\text{m}$ , CO is prominent at  $2.3 \mu\text{m}$ , and FeH is present at 0.99, 1.2, and  $1.6 \mu\text{m}$ . The  $J$ -band spectral region exhibits a number of features that can be attributed to  $K I$  and  $Na I$  lines, in addition to FeH. There is no indication of  $CH_4$  in the spectrum of this source. These features are all indicative of a late-type L dwarf, as also indicated by the optical spectrum of Cruz et al. (2007).

TABLE 2  
2M 2132+1341AB OBSERVED PROPERTIES

Property	Measurement
$\Delta J$ .....	$0.84 \pm 0.09$ mag
$\Delta H$ .....	$0.88 \pm 0.04$ mag
$\Delta K_s$ .....	$0.90 \pm 0.04$ mag
$J_A$ .....	$16.07 \pm 0.07$ mag
$J_B$ .....	$16.91 \pm 0.12$ mag
$(J-K_s)_A$ .....	$1.84 \pm 0.09$ mag
$(J-K_s)_B$ .....	$1.78 \pm 0.14$ mag
$(J-H)_A$ .....	$1.04 \pm 0.09$ mag
$(J-H)_B$ .....	$1.00 \pm 0.13$ mag
Separation.....	$66 \pm 4$ mas
Position angle.....	$121.94^\circ \pm 1.30^\circ$
Date observed.....	UT 2006 Jun 17

NOTE.—Photometry on the MKO system.

### 3. ANALYSIS

The key binary properties of 2M 2132+1341AB are derived here and summarized in Table 3. Individual apparent magnitudes are calculated from the observed  $\Delta$  magnitudes (Table 2) and the integrated apparent magnitudes (unresolved) measured by the Two Micron All Sky Survey (2MASS; Cutri et al. 2003). Since the differential photometry observed with NIRC2 was measured with the MKO filter system, we converted the integrated  $J$  and  $H$  photometry from the 2MASS filter system to MKO using the color transformations of Leggett et al. (2007). While they provide no transformation between  $K_s$  MKO and  $K_s$  2MASS, the transmission curves are very similar (1%–2% difference; S. Leggett 2006, private communication) and therefore we apply no correction. Uncertainties in the transformations and photometry are propagated in quadrature and reported in Table 3.

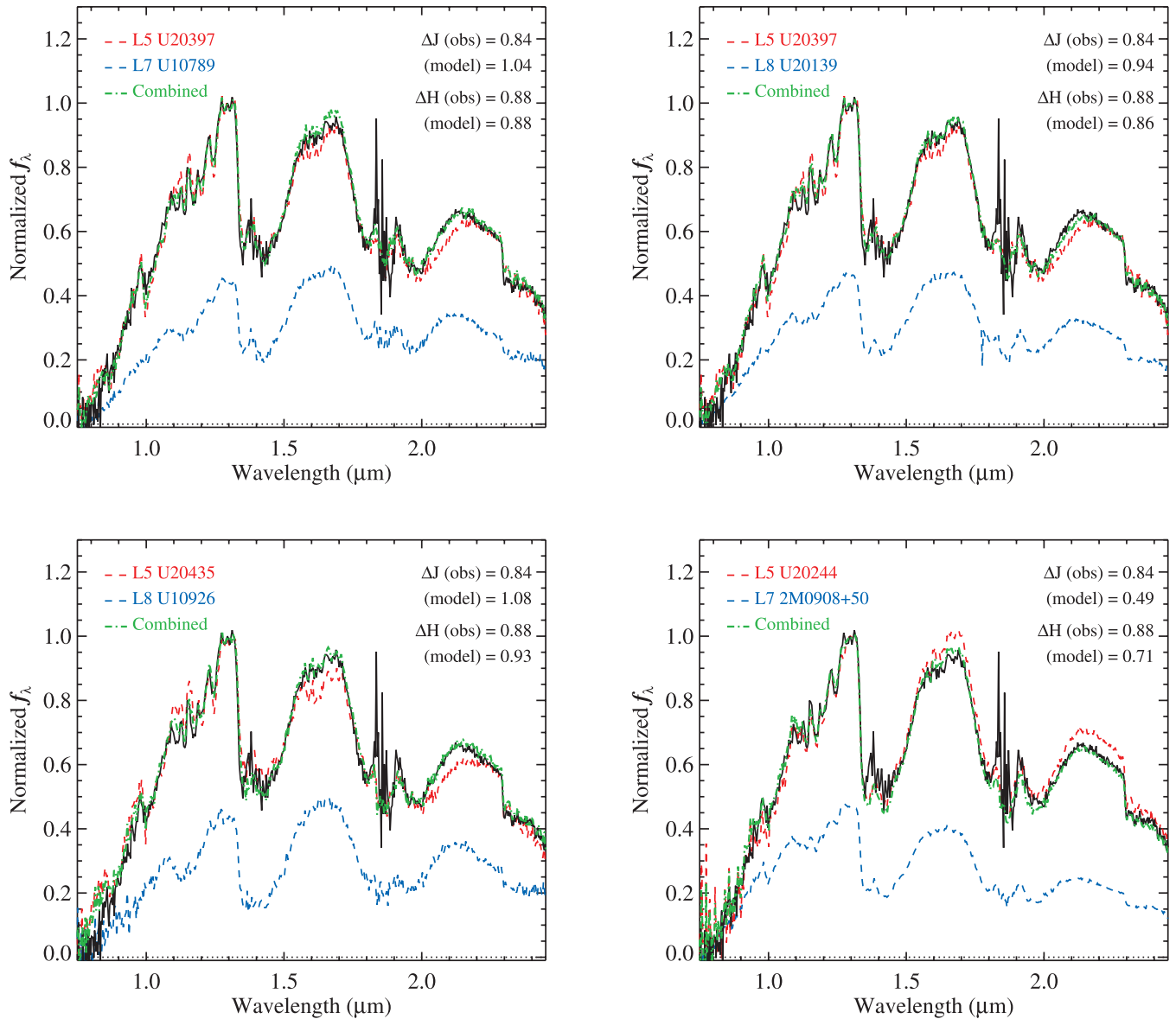


FIG. 2.—Comparisons between the observed spectrum of 2M 2132+1341AB and the composite spectra made by combining IRTF SpeX spectra of spectral templates. In each panel, the observed near-infrared spectrum is represented by the black line. The upper (red dashed line) and lower (blue dashed line) spectra in each panel are template guesses of the primary and secondary, respectively. The combined spectrum is represented by the green dot-dashed line. The  $K$  flux ratios between the secondary and primary are set to 2.29 ( $\Delta K = 0.9$  mag) in each composite spectrum. The corresponding magnitude differences of the fits at  $\Delta J$  and  $\Delta H$  are shown in each panel. The two top panels and the bottom left panel suggest that an L5/L7.5 composite gives the closest match morphologically to the integrated 2M 2132+1341AB spectrum at  $J$  and  $H$ . We include the bottom right panel to demonstrate that this kind of analysis is sufficiently robust to remove atypical component spectra (an atypically red L5 and an atypically blue L7), even when there is good morphological matching; see § 3.1.

With measured differential photometry, derived apparent magnitudes, and a measured combined  $L6 \pm 0.5$  optical spectrum from Cruz et al. (2007), what physical properties of the individual components can we infer? Since there is no known trigonometric parallax for the object, we rely on first estimating the component spectral types to derive absolute magnitudes using an empirical relation. This then enables estimates of the distance modulus, bolometric luminosities, and ultimately, with the aid of theoretical evolutionary tracks, masses and a period. The better constrained the component spectral types are, the more constrained (and meaningful) will be the derived physical properties.

### 3.1. Spectral Types

The component near-infrared colors listed in Table 2 by themselves provide only rough constraint on the individual spectral

types (e.g., Chiu et al. 2006). While the primary is certainly a mid-L dwarf, L3–L8, the possible spectral types for the secondary extend into the T range, L3–T1. While the combined light spectrum is similar to that of an L6, the components may have very discrepant spectral types. The secondary could even be a T dwarf without the characteristic  $\text{CH}_4$  bands appearing in the combined light spectrum.

To derive more precise estimates of the individual component spectral types, we used a spectral synthesis technique based on that used by Burgasser et al. (2006b) to study L dwarf plus T dwarf binaries.<sup>11</sup> A large sample of composite spectra was generated

<sup>11</sup> See also Cruz et al. (2004), Burgasser et al. (2005b), Liu et al. (2006) and Reid et al. (2006).

TABLE 3  
2M 2132+1341AB DERIVED PROPERTIES

Property	Value
Spectral Types	
A+B (optical).....	L6 ± 1
A.....	L5 ± 0.5
B.....	L7.5 ± 0.5
$M_{K_A}$ .....	11.92 ± 0.33 mag
$M_{K_B}$ .....	12.82 ± 0.30 mag
Distance.....	28 ± 4 pc
Luminosities	
$L_A$ .....	$(6.3 \times 10^{-5}) \pm (1.9 \times 10^{-5}) L_{\odot}$
$L_B$ .....	$(3.0 \times 10^{-5}) \pm (1.0 \times 10^{-5}) L_{\odot}$
Masses (A/B)	
0.8 Gyr.....	0.065/0.048 $M_{\odot}$
5 Gyr.....	0.077/0.075 $M_{\odot}$
10 Gyr.....	0.078/0.076 $M_{\odot}$
Proper Motion (NOMAD)	
$\mu_{\alpha} \cos \delta$ .....	-55.3 ± 9.0 mas yr <sup>-1</sup>
$\mu_{\delta}$ .....	-394.7 ± 9.0 mas yr <sup>-1</sup>
Separation (projected).....	1.8 ± 0.3 AU
Orbital period.....	7–12 yr

NOTES.—All photometry is on the MKO filter system. See § 3 for details and references.

by combining various pairings of L5–T6 SpeX prism spectra obtained by A. Burgasser & K. Cruz (72 individual spectra in all). The spectral types of the template spectra are based on optical classifications for L dwarfs (e.g., Kirkpatrick et al. 1999) and near-infrared classifications for the T dwarfs (e.g., Burgasser et al. 2006b). The components of these spectra were constrained to have the same relative  $K_s$ -band magnitudes as measured for 2M 2132+1341AB and to simultaneously be within  $3\sigma$  of the measured  $\Delta J$  (0.27 mag) and  $\Delta H$  (0.12 mag). The best matches between the composite spectra and the observed (unresolved) spectrum of 2M 2132+1341AB were quantitatively determined by comparing both relative  $J$  and  $H$  magnitudes and  $H_2O$  and  $CH_4$  spectral ratios (defined in Burgasser et al. 2006a). No assumption was made on the absolute magnitudes of the individual components in this analysis, so the absolute magnitude/spectral type scale was left as a free parameter.

Figure 2 illustrates the three best-fit composite spectra based on both the relative magnitudes and spectral ratio comparisons. In all three cases, an L5 spectral classification is selected for the primary, along with an L7 or L8 for the secondary. In fact, this was the case for the best 20 fits. While the uncertainty is dominated by one subclass of uncertainties in the individual library spectral classifications, the consistency in the matches likely averages out the overall uncertainty. Hence, we conclude that the primary is a likely L5 ± 0.5 and its companion a likely L7.5 ± 0.5.

The fourth fit shown in Figure 2 (*bottom right*) shows one of the combinations that was disqualified due to the disparity between the predicted and measured  $\Delta$  magnitudes. The components of this system are the unusually red L5 2MASS J062445.95–452154.8 (I. N. Reid et al. 2007, in preparation) and the unusually blue L7 2MASS J09083803+5032088 (Cruz et al. 2003, 2007). Despite a good morphological fit, this kind of analysis that includes

$\Delta$  magnitudes as constraints to the properties of individual components is sufficiently robust to remove atypical component spectra. Of course, resolved near-infrared spectroscopy is required to verify the accuracy of these classifications.

### 3.2. Physical Companions?

Are the components of 2M 2132+1341AB physical companions? Calculating spectrophotometric distances of the two sources separately results in equal values,  $28 \pm 4$  pc. We used the fitted spectral types to independently obtain intrinsic flux densities ( $M_K$ ) from the polynomial fit of Burgasser (2007). The distance's uncertainty includes those in the spectral types and in a spectral type/absolute magnitude relation (see § 3.3) taken in quadrature. In addition, assuming a surface density of order  $10^{-3} \text{ deg}^{-2}$  (Cruz et al. 2007) for all nearby L dwarfs, the probability of two lying within  $0.1''$  is  $\approx 10^{-7}$ . Hence, random alignment is very unlikely. Finally, the 2M 2132+1341 pair, or at least the primary, shows a large proper motion of  $0.4'' \text{ yr}^{-1}$  (NOMAD astrometric catalog; Zacharias et al. 2004). A 2MASS  $K_s$  image of 2M 2132+1341 observed in UT 1998 appears single. With sensitivity to point-source brightness of  $K_s \approx 15.3$  mag, 2M 2132+1341B would have been detectable and resolved at separations  $\geq 1.5''$  (Burgasser et al. 2005a). Therefore, we rule out 2M 2132+1341B as an unrelated background object, since its projected position nearly 8 years ago would have been resolved in the 2MASS image. These factors provide strong evidence that the two sources are physical companions.

### 3.3. Masses, Age, and Period

With well-constrained spectral types in hand, we can now derive many of the binary's physical properties summarized in Table 3. An absolute  $K$  magnitude for the primary is obtained using an  $M_K$ -spectral type relation from Figure 3 of Burgasser (2007), in which binaries have been excluded. The companion absolute magnitude is then obtained by applying our measured  $\Delta K_s$  ( $\approx \Delta K$ ; S. Leggett 2006, private communication). Using our constrained component spectral types, we acquire the  $K$ -band bolometric corrections from Golimowski et al. (2004), apply them to our  $\Delta K$  photometry, and calculate the bolometric luminosity ratio between the components to be  $0.32 \pm 0.08$  dex. Individual bolometric luminosities in units of solar luminosity, estimated from the component  $M_K$  and  $(BC)_K$  values, are  $(6.3 \times 10^{-5}) \pm (1.9 \times 10^{-5}) L_{\odot}$  for the primary and  $(3.0 \times 10^{-5}) \pm (1.0 \times 10^{-5}) L_{\odot}$  for the companion.

Individual masses of 2M 2132+1341A and B can be estimated from theoretical evolutionary models using our derived bolometric luminosities and estimated ages of the system. The system's age, however, is less constrained. The binary does not appear affiliated with any moving group or open cluster. Its optical spectrum shows no lithium or  $H\alpha$  spectral features (Cruz et al. 2007), suggesting that the source is more consistent with old field L dwarfs (Kirkpatrick et al. 2000; West et al. 2004); nor is there any near-infrared color or optical spectrum evidence of sub-solar metallicity (e.g., Burgasser et al. 2003, 2004), indicating that the system is probably not a member of the Galaxy's thick disk or halo populations ( $\geq 10$  Gyr; Reid & Hawley 2005). In addition, the system's tangential motion of  $53 \pm 2 \text{ km s}^{-1}$  (NOMAD; Zacharias et al. 2004) is inconsistent with a young object ( $\lesssim 1$  Gyr).

The lack of lithium absorption in the optical spectrum can help place a lower mass limit to 2M 2132+1341A of approximately  $0.065 M_{\odot}$ , depending on the system's age (Rebolo et al. 1992; Chabrier et al. 1996; Basri et al. 1996; Burrows et al. 1997). Objects

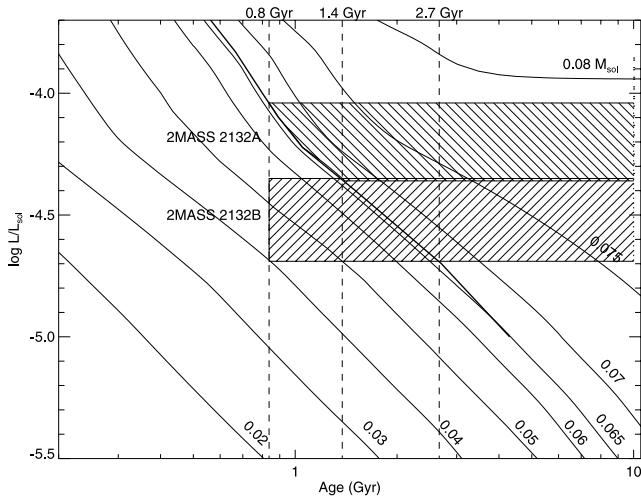


FIG. 3.—Theoretical evolutionary tracks from Burrows et al. (1997) for 2M 2132+1341A (upper hatched region) and B (lower hatched region). Diagonal solid lines show constant-mass tracks; labeled numbers are in solar mass units. The stellar/substellar boundary for the model is  $\approx 0.075 M_{\odot}$ ; the thick solid line represents the 1% lithium depletion boundary drawn between the ages of 0.55 and 4.5 Gyr. The lack of a lithium absorption feature in the combined optical spectrum (Cruz et al. 2007) suggests ages to the right of this line ( $\geq 0.8$ –1.3 Gyr). Based on derived luminosity ranges and estimated upper age limits discussed in § 3.3, the two hatched regions predict possible primary masses of  $0.065$ – $0.078 M_{\odot}$  and companion masses of  $0.040$ – $0.077 M_{\odot}$ .

with less than this limiting mass will always have central temperatures below the lithium-burning temperature. Slightly more massive objects will undergo lithium burning such that the element is observable at only younger ages. For example, using the models of Burrows et al. (1997) a  $0.075 M_{\odot}$  object will undergo complete lithium burning in about 140 Myr. In Figure 3 we show their theoretical evolutionary tracks, and we place the lower mass limit of 2M 2132+1341A along a constant lithium abundance line of 1% of the original abundance (similar to Liu & Leggett [2005], we assume that a decrease in the initial lithium abundance by a factor of 100 marks the lithium absorption detection limit). This provides a lower age limit of 0.8–1.3 Gyr, consistent with a weak or absent lithium absorption feature. Assuming that the companion is coeval with the primary, this lower age along with the uncertainties in the secondary’s luminosity predicts masses of  $0.040$ – $0.054 M_{\odot}$ . A 10 Gyr upper limit results in a primary mass of  $0.077$ – $0.079 M_{\odot}$  and a secondary of  $0.076$ – $0.077 M_{\odot}$ . According to a theoretical analysis conducted by Allen et al. (2005) of the age distribution of nearby field L dwarfs, there is a  $\sim 30\%$  probability that 2M 2132+1341A and B are less than  $\sim 1$  Gyr old and a  $\sim 75\%$  chance that they are younger than  $\sim 5$  Gyr. We list the median mass estimates for three ages in Table 3, including a 5 Gyr best guess for stars in the solar neighborhood. Both objects likely straddle the hydrogen-burning mass threshold ( $\approx 0.072$ – $0.075 M_{\odot}$ ; Burrows et al. 1997; Baraffe et al. 1998), with the secondary being most likely substellar.

The projected separation between the two components is only  $1.8 \pm 0.3$  AU (at a distance of  $28 \pm 4$  pc). We estimate the semi-major axis of 2M 2132+1341AB by assuming that on average the true semimajor axis is 1.26 times larger than the projected separation (Fischer & Marcy 1992) or  $\langle a \rangle = 2.3$  AU. Using Kepler’s third law and the range of possible masses, we estimate an orbital period of 7–12 yr. Hence, this system is a good candidate target for astrometric monitoring to derive orbital mass measurements (Lane et al. 2001; Bouy et al. 2004; Zapatero Osorio et al. 2004).

## 4. DISCUSSION

### 4.1. How Typical Are the Binary Properties of 2M 2132+1341AB?

Very low mass (VLM) binaries are characterized by near-unity mass ratios ( $q \sim 0.8$ – $1.0$ ) and tight separation distributions peaking between 3 and 10 AU (Burgasser et al. 2007 and references within). According to the Very Low Mass Binaries Archive,<sup>12</sup> about a third of these systems are L/L binaries. The binary properties of 2M 2132+1341AB,  $q \gtrsim 0.9$  and projected separation of  $1.8 \pm 0.3$  AU, are consistent with these distributions.

Currently, there are 16 known VLM binaries with angular separations less than the mean 66 mas separation of 2M 2132+1341AB. The tightest nine are spectroscopic binaries and are as yet unresolved. The subsequent seven were all discovered with the *HST*. Despite large-aperture ground-based telescopes achieving AO-corrected resolutions at *K* of typically twice that of the *HST*, the space telescope’s more stable PSF allows for the identification of undersampled binaries. It is interesting to note that 2M 2132+1341AB is the tightest resolved VLM binary discovered by a ground-based telescope, and the tightest using LGS AO. The clear separation of this system into two well-resolved components indicates that with good AO correction, ground-based facilities can indeed achieve a superior resolution in the near-infrared compared to *HST*.

### 4.2. Future Dynamical Mass for 2M 2132+1341AB

Theoretical evolutionary models of mass-luminosity-age relations are still largely uncalibrated for the lowest mass objects. In fact, only three VLM systems with constrained ages (all young) have had reliable orbits and resolved fluxes, leading to derived individual kinematic masses: AB Dor C ( $\sim 50$ – $100$  Myr; Close et al. 2005; Luhman et al. 2005), the eclipsing brown dwarf binary 2MASS J05352184–0546085AB found in Orion ( $\sim 1$ – $2$  Myr; Stassun et al. 2006), and GJ 569Bab ( $\sim 500$  Myr; Zapatero Osorio et al. 2004). Unfortunately, neither 2M 2132+1341AB’s age nor distance is sufficiently well constrained to be used as a high-accuracy luminosity-mass calibrator. However, if future high-resolution optical spectroscopy (e.g., repaired Space Telescope Imaging Spectrograph on *HST*) shows the presence of lithium in the companion, the system’s age could be further constrained to  $\sim 0.8$ – $2.5$  Gyr, making it a useful system for dynamical mass measurements. This would likely require, however, a widening in the components’ projected separation. The *HST* and/or ground-based LGS AO observations should be able to measure significant orbital motion over the next  $\sim 6$  yr, similar to the study of 2MASSW J0746425+2000321 (Bouy et al. 2004), the only dynamical mass measurement of an L dwarf binary.

## 5. SUMMARY

Keck II LGS AO observations of 2MASS J21321145+1341584 show that this very low mass dwarf is a binary system. Observed differential near-infrared photometry and integrated spectra (optical and near-infrared) indicate that both components are consistent with mid-L dwarfs. Based on modeling the integrated optical spectra with spectra from 72 known L and T dwarfs, we identify 2M 2132+1341A as an  $L5 \pm 0.5$  and 2M 2132+1341B as an  $L7.5 \pm 0.5$ . The lack of lithium in the optical spectra suggests

<sup>12</sup> The archive lists all the VLM binary systems reported in refereed journals, defined as binaries with total estimated mass less than  $\sim 0.2 M_{\odot}$ . This mass limit is arbitrary and corresponds to binary M6 field dwarfs (slightly earlier spectral types for younger objects). The Web site is maintained by Nick Siegler at [http://paperclip.as.arizona.edu/~nsiegler/VLM\\_binaries](http://paperclip.as.arizona.edu/~nsiegler/VLM_binaries).

that the primary's age is older than 800 Myr. The system's very close separation ( $0.066''$ ) and common proper motion from 2MASS infers a physical association. With a conservative age estimate of 5 Gyr, model-dependent masses suggest a system whose components straddle the hydrogen-burning limit threshold, with the primary likely stellar and the secondary likely substellar. The close projected separation ( $1.8 \pm 0.3$  AU) and near-unity mass ratio of the system are consistent with previous results for field VLM binaries. The relatively short estimated orbital period of this system ( $\sim 7$ – $12$  yr) makes it an ideal target for dynamical mass measurements. At the time of this writing, 2M 2132+1341AB's angular separation is the tightest for any VLM binary discovered from a ground-based telescope and is the tightest using LGS AO.

The authors would like to acknowledge NASA and the NASA Time Allocation Committee for making this time available and the entire Keck LGS AO team for having set the bar for LGS performance. We also thank the referee Kevin Luhman for a thorough

reading and suggested improvements. N. S. would like to thank Mike Cushing for discussions regarding L and T spectral classifications and Adam Burrows for providing model calculations. C. M. and B. M. note that their research was performed under the auspices of the US Department of Energy by the University of California, Lawrence Livermore National Laboratory, under contract W-7405-ENG-48, and also supported in part by the NSF Science and Technology Center for AO, managed by the University of California at Santa Cruz, under cooperative agreement AST 98-76783. This research has made use of the Simbad and VizieR databases operated at CDS in Strasbourg, France; the 2MASS data services, a joint project of the University of Massachusetts and the Infrared Processing and Analysis Center/California Institute of Technology, funded by NASA and the NSF; the US Naval Observatory (USNO) Naval Observatory Merged Astrometric Dataset (NOMAD). IRAF is distributed by the National Optical Astronomy Observatory, which is operated by the Association of Universities for Research in Astronomy, Inc., under contract to the NSF.

## REFERENCES

- Allen, P. R., Kroener, D. W., Reid, I. N., & Trilling, D. E. 2005, *ApJ*, 625, 385  
 Baraffe, I., Chabrier, G., Allard, F., & Hauschildt, P. H. 1998, *A&A*, 337, 403  
 Basri, G., Marcy, G. W., & Graham, J. R. 1996, *ApJ*, 458, 600  
 Becklin, E. E., & Zuckerman, B. 1988, *Nature*, 336, 656  
 Bouchez, A. H., et al. 2004, *Proc. SPIE*, 5490, 321  
 Bouy, H., et al. 2004, *A&A*, 423, 341  
 Burgasser, A. J. 2004, *ApJ*, 614, L73  
 ———. 2007, *ApJ*, 659, 655  
 Burgasser, A. J., Geballe, T. R., Leggett, S. K., Kirkpatrick, J. D., & Golimowski, D. A. 2006a, *ApJ*, 637, 1067  
 Burgasser, A. J., Kirkpatrick, J. D., & Lowrance, P. J. 2005a, *AJ*, 129, 2849  
 Burgasser, A. J., Reid, I. N., Leggett, S. K., Kirkpatrick, J. D., Liebert, J., & Burrows, A. 2005b, *ApJ*, 634, L177  
 Burgasser, A. J., Reid, I. N., Siegler, N., Close, L. M., Allen, P., Lowrance, P. J., & Gizis, J. E. 2007, in *Planets and Protostars V*, ed. B. Reipurth, D. Jewit, & K. Keil (Univ. Arizona Press: Tucson), 427  
 Burgasser, A. J., et al. 2003, *ApJ*, 592, 1186  
 ———. 2006b, *ApJS*, 166, 585  
 Burrows, A., et al. 1997, *ApJ*, 491, 856  
 Chabrier, G., Baraffe, I., & Plez, B. 1996, *ApJ*, 459, L91  
 Chiu, K., et al. 2006, *AJ*, 131, 2722  
 Close, L. M., et al. 2002, *ApJ*, 566, 1095  
 ———. 2005, *Nature*, 433, 286  
 ———. 2007, *ApJ*, in press  
 Cruz, K. L., Reid, I. N., Liebert, J., Kirkpatrick, J. D., & Lowrance, P. J. 2003, *AJ*, 126, 2421  
 Cruz, K. L., et al. 2004, *ApJ*, 604, L61  
 ———. 2007, *AJ*, 133, 439  
 Cushing, M. C., & Vacca, W. D. 2006, *AJ*, 131, 1797  
 Cushing, M. C., Vacca, W. D., & Rayner, J. T. 2004, *PASP*, 116, 362  
 Cutri, R. M., et al. 2003, 2MASS All-Sky Data Release Point Source Catalog (Pasadena: IPAC), <http://tdc-www.harvard.edu/software/catalogs/tmpsc.html>  
 Dahn, C. C., et al. 2002, *AJ*, 124, 1170  
 Fischer, D. A., & Marcy, G. W. 1992, *ApJ*, 396, 178  
 Gelino, C. R., Kulkarni, S. R., & Stephens, D. C. 2006, *PASP*, 118, 611  
 Golimowski, D. A., et al. 2004, *AJ*, 127, 3516  
 Hawley, S. L., et al. 2002, *AJ*, 123, 3409  
 Kirkpatrick, J. D. 2005, *ARA&A*, 43, 195  
 Kirkpatrick, J. D., Henry, T. J., & Simons, D. A. 1995, *AJ*, 109, 797  
 Kirkpatrick, J. D., et al. 1999, *ApJ*, 519, 802  
 ———. 2000, *AJ*, 120, 447  
 Lane, B. F., Zapatero Osorio, M. R., Britton, M. C., Martín, E. L., & Kulkarni, S. R. 2001, *ApJ*, 560, 390  
 Leggett, S. K., et al. 2007, *MNRAS*, in press  
 Lépine, S., Rich, R. M., & Shara, M. M. 2003, *ApJ*, 591, L49  
 Liu, M. C. 2006, *Proc. SPIE*, 6272, 6272OH  
 Liu, M. C., & Leggett, S. K. 2005, *ApJ*, 634, 616  
 Liu, M. C., et al. 2006, *ApJ*, 647, 1393  
 Luhman, K. L., Stauffer, J. R., & Mamajek, E. E. 2005, *ApJ*, 628, L69  
 Monet, D. G., et al. 2003, *AJ*, 125, 984  
 Nakajima, T., Oppenheimer, B. R., Kulkarni, S. R., Golimowski, D. A., Matthews, K., & Durrance, S. T. 1995, *Nature*, 378, 463  
 Oppenheimer, B. R., Kulkarni, S. R., Matthews, K., & Nakajima, T. 1995, *Science*, 270, 1478  
 Rayner, J. T., Toomey, D. W., Onaka, P. M., Denault, A. J., Stahlberger, W. E., Vacca, W. D., Cushing, M. C., & Wang, S. 2003, *PASP*, 115, 362  
 Rebolo, R., Martín, E. L., & Magazzu, A. 1992, *ApJ*, 389, L83  
 Reid, I. N., & Hawley, S. L. 2005, *New Light on Dark Stars* (2nd ed.; Chichester: Praxis Publishing)  
 Reid, I. N., Lewitus, E., Allen, P. R., Cruz, K. L., & Burgasser, A. B. 2006, *AJ*, 132, 891  
 Roddier, F. 2004, *Adaptive Optics in Astronomy* (Cambridge: Cambridge Univ. Press)  
 Siegler, N., Close, L. M., & Freed, M. 2003, *Proc. SPIE*, 4839, 114  
 Simons, D. A., & Tokunaga, A. 2002, *PASP*, 114, 169  
 Stassun, K. G., Mathieu, R. D., & Valenti, J. A. 2006, *Nature*, 440, 311  
 Tokunaga, A., Simons, D. A., & Vacca, W. D. 2002, *PASP*, 114, 180  
 Vacca, W. D., Cushing, M. C., & Rayner, J. T. 2003, *PASP*, 115, 389  
 West, A. A., et al. 2004, *AJ*, 128, 426  
 Wizinowich, P. L., et al. 2004, *Proc. SPIE*, 5490, 1  
 ———. 2006, *PASP*, 118, 297  
 Zacharias, N., Monet, D. G., Levine, S. E., Urban, S. E., Gaume, R., & Wycoff, G. L. 2004, *BAAS*, 36, 1418  
 Zapatero Osorio, M. R., Lane, B. F., Pavlenko, Y., Martín, E. L., Britton, M., & Kulkarni, S. R. 2004, *ApJ*, 615, 958